Characterization of Parotid Tumors With Dynamic Susceptibility Contrast Perfusion-Weighted Magnetic Resonance Imaging and Diffusion-Weighted MR Imaging

Ahmed Abdel Khalek Abdel Razek, MD, Sieza Samir, MD, and Germeen Albair Ashmalla, MD

Purpose: To characterize parotid tumors with dynamic susceptibility contrast perfusion-weighted magnetic resonance (MR) imaging and diffusion-weighted MR imaging.

Material and Methods: Prospective study was conducted upon 48 consecutive patients (27 men, 21 women; aged 15–75 years; mean, 45 years) with parotid tumors that underwent dynamic susceptibility contrast perfusion-weighted MR imaging was performed after bolus injection of gadopentate dimeglumine and diffusion-weighted MR imaging. The dynamic susceptibility contrast percentage (DSC%) and apparent diffusion coefficient (ADC) values of parotid tumors were calculated and correlated with histopathological findings.

Results: The DSC% of malignant parotid tumors (33.53% ± 3.99%) was significantly different (P = 0.001) from that of benign parotid tumors (22.29% ± 4.13%). The threshold values of DSC% and ADC used in differentiating malignant from benign parotid tumors were 26.5% and 1.07×10^{-3} mm^2/s, respectively, with area under the curve (AUC) of 0.96 and 0.81, respectively. The DSC% of malignant parotid tumors was significantly different from that of Warthin tumors (P = 0.001). The cutoff DSC% used to differentiate malignancy from Warthin tumors was 26.9% with an AUC of 0.99. There was a significant difference in DSC% and ADC values between pleomorphic adenomas and Warthin tumors (P = 0.001). The threshold values of DSC% and ADC used in differentiating pleomorphic adenomas from Warthin tumors was 22.5% and 0.99×10^{-3} mm^2/s, respectively, with AUC of 0.88 and 0.98, respectively.

Conclusions: Dynamic susceptibility contrast-enhanced perfusion-weighted MR imaging and diffusion-weighted MR imaging are noninvasive promising methods that are used for differentiation of malignant from benign parotid tumors and for characterization of some benign parotid tumors.

Key Words: diffusion, perfusion, MR imaging, parotid, tumor

(*J Comput Assist Tomogr* 2017;41: 131–136)

Characterization of parotid tumors is important for preoperative treatment planning. The surgery chosen for treatment of parotid tumors depends on the histologic type of the tumor. When the tumor is malignant, total parotidectomy is selected, and the facial nerve may be sacrificed.[1–3] Routine ultrasound and advanced ultrasound elastography are used initially for assessment of parotid tumors, but their results are overlapping.[4–6] Postcontrast-computed tomography and perfusion-computed tomography has a role in assessment of parotid tumors, but it is eradicated with radiation exposure and contrast medium injection.[7,8] Conventional magnetic resonance (MR) imaging have been used for anatomical and morphological assessment of parotid tumors. Unfortunately, this information is not sufficient for the surgeons, and additional functional data are still required for better characterization of parotid tumors.[9] Advanced MR imaging sequences, such as dynamic contrast-enhanced MR imaging[10,11] and MR spectroscopy are used but their parameters are often overlapping.[12,13] Fine-needle aspiration cytology is widely used for evaluation of parotid asses. However, the results of cytology may be inconclusive or even false, owing to insufficient samples and small tumor size.[1–3]

Dynamic susceptibility contrast perfusion-weighted MR imaging is used to track the first pass of an exogenous, paramagnetic, contrast agent through tissues, and has emerged as a powerful tool in the characterization of tumor hemodynamics.[14–17] This sequence use snapshot imaging, such as echo-planar imaging to follow the first pass of an injected contrast agent, allowing for the acquisition of baseline data prior to arrival of the bolus. The passage of injected contrast agent through the tissue results in loss of MR signal intensity, which is related to the concentration of contrast agent in the tissue.[15–18] Dynamic susceptibility contrast perfusion-weighted MR imaging can be helpful in grading of brain tumors, prediction of treatment response, differentiation between tumor recurrence, and radiation necrosis.[14–16] This technique was used for assessment of head and neck tumors, characterization of cervical lymph nodes, and differentiation of recurrent head and neck cancer from postradiation changes.[15–19] Diffusion-weighted MR imaging shows overlap in the apparent diffusion coefficient (ADC) of benign and malignant parotid tumors.[20–25] To our knowledge, there is no previous studies in the literature had explored the usefulness of dynamic susceptibility contrast perfusion-weighted imaging in the evaluation of parotid gland tumors.

The aim of this work is to characterize parotid tumors with dynamic susceptibility contrast perfusion-weighted MR imaging and diffusion-weighted MR imaging.

MATERIALS AND METHODS

Patients and Methods

We obtained institutional review board approval and an informed consent from the patients before the study. This prospective study was conducted on 51 consecutive patients with clinical and/or sonographic diagnosis of solid parotid masses. Three patients were excluded from the study: 1 patient whose lesion turned on to be cystic, 1 patient with significant motion artifact degrading the quality of the images and a third patient with poor image quality due to susceptibility artifacts. A total of 48 patients (27 men and 21 women) were qualified for the final analysis of the study. They presented clinically with: parotid mass (n = 38), facial pain (n = 20), and facial palsy (n = 19). The patient age ranged between 15 and 75 years (mean, 45 years). The final

From the Department of Diagnostic Radiology, Mansoura Faculty of Medicine, Mansoura, Egypt.
Received for publication March 23, 2016; accepted May 16, 2016.
Correspondence to: Ahmed Abdel Khalek Abdel Razek, MD, Diagnostic Radiology Department, Mansoura Faculty of Medicine, Mansoura 13551, Egypt (e-mail: arazek@mans.edu.eg).
The authors declare no conflict of interest.

DOI: 10.1097/RCT.0000000000000486

diagnosis of the parotid tumors was confirmed by biopsy in all patients. Biopsy included fine-needle aspiration biopsy in 18 patients and surgical biopsy in 30 lesions. The biopsy or surgery was done for all patients within 5 to 15 days after the MR imaging. All patients underwent routine T1- and T2-weighted MR imaging, diffusion-weighted MR imaging, dynamic susceptibility perfusion-weighted MR imaging and finally routine postcontrast T1-weighted images of the parotid gland.

Routine MR Imaging

The MR studies were performed on a 1.5 Tesla scanner (Symphony; Siemens Medical Systems, Erlangen, Germany) equipped with a self-shielding gradient set (maximum gradient strength = 30 mT and slew rate = 120 T/m/s). A circularly polarized head coil and a standard 2-element circularly polarized neck array coil were used for all patients. The flexibility of the neck array coil allowed positioning of the N1 element (the upper part of the coil) right next to the parotid glands. Initially, for anatomic localization of the parotid gland, an axial T1-weighted spin-echo sequence (repetition time/echo time [TR/TE] = 500/14 ms) was performed by using a matrix, 192 × 512; field of view (FOV), 20–25 cm, a section thickness of 5 mm with an interslice gap of 1.25 mm, and 3 signals averaged. Transverse T2-weighted MR images were obtained with TR/TE, 2800/96 ms; FOV, 20–25 cm; section thickness, 5 mm; interslice gap, 1–2 mm; and matrix, 320 × 180.

Diffusion-Weighted MR Imaging

Diffusion-weighted MR imaging was performed by using a multislice echo-planar (EPI) single-shot spin-echo sequence, in the transverse plane (TR/TE = 3200/118 ms, FOV = 20–25 cm, matrix =128 × 128, section thickness = 5 mm and interslice gap = 2). Three diffusion gradients were applied sequentially in the x, y, and z directions with b values of 0, 500, and 1000 s/mm^2. The acquisition time was 48 seconds. The ADC maps were automatically generated.

Perfusion-Weighted MR Imaging

Multi-slice echo-planar imaging gradient echo sequence was used. The scanning parameters were as follows: TR/TE, 2280/47 ms; number of excitation, 1; flip angle, 80 degrees; slice thickness, 5 mm; interslice gap, 1.5 mm; FOV, 20–25 cm; and matrix, 128 × 128. Dynamic susceptibility contrast T2*-weighted perfusion-weighted MR images were obtained after the administration of a bolus of gadopentate dimegulumine in a dose of 0.1 mmol/kg body weight. The contrast was injected using an automatic injector at a rate of 5 mL/s, and this was followed by the injection of 20-mL saline. The gadolinium was administrated in all patients after the acquisition of baseline data for about 8 seconds. The data acquisition time was 110 seconds, and the time between the data points was 2 seconds. After the dynamic contrast study, a series of axial, sagittal, and coronal postcontrast T1-weighted images were obtained for all patients.

Image Analysis

Image analysis was performed by 1 radiologist (S.S.) expert in MR imaging for 20 years who was blinded to the clinical diagnosis. The circular region of interest (ROI) was placed at dynamic susceptibility image around the margins of a homogenously enhancing parotid mass using an electronic cursor. When heterogeneity of the signal intensity within the mass was observed, an ROI was placed around the enhanced solid part of the tumor avoiding the cystic or necrotic parts of the tumor guided by the contrast enhanced MR imaging results. In patients with bilateral or multiple lesions, the ROI was placed around the largest lesion only. Postprocessing of the images was done to obtain the time signal intensity curve for the lesion. The dynamic susceptibility contrast percentage (DSC%) was calculated with the following equation: maximum signal intensity loss = unenhanced lesion signal intensity (S0) − maximum contrast enhanced signal intensity (SI)/unenhanced lesion signal intensity (S0) × 100%.[18,19] A copy of ROI was placed on the ADC map with calculation of the ADC value of the tumor.

Statistical Analysis

Statistical analysis was done by using statistical package for social science (SPSS) software package for windows version 20. One-way analysis of variance test was done to compare more than 2 groups and Student *t* test to compare between 2 groups. A value of *P* less than 0.05 was considered as being significant. We used receiver operating characteristic curves to determine the cut off values of DSC% and ADC which can be used in differentiation of malignant from benign parotid tumors, Warthin tumors from malignant tumors and Warthin tumors from pleomorphic adenomas. The sensitivity, specificity, accuracy and area under the curve (AUC) for the DSC% and ADC values were calculated, for each group.

RESULTS

Demographic Analysis

The final pathological diagnosis of the parotid gland tumors were: pleomorphic adenoma (Fig. 1) (n = 16), Warthin tumor (Fig. 2) (n = 10), monomorphic adenoma (n = 2), neurofibroma (n = 2), mucoepidermoid carcinoma (Fig. 3) (n = 8), adenoid cystic carcinoma (n = 2), carcinoma ex adenoma (n = 2), lymphoma (n = 4), and metastasis (n = 2). Table 1 shows the mean, standard deviation, minimum and maximum DSC% and ADC values of benign and malignant tumors.

The mean DSC% of malignant parotid tumors (33.53% ± 3.99) was significantly different ($P = 0.001$) from that of benign tumors (22.29% ± 4.13). The mean ADC value of malignant parotid tumors ($0.94 \pm 0.20 \times 10^{-3}$ mm^2/s) was significantly different ($P = 0.001$) from that of benign tumors ($1.22 \pm 0.22 \times 10^{-3}$ mm^2/s). When a DSC% of 26.5 % was used as a threshold value for differentiating malignant from benign parotid tumors, the best results were obtained with an accuracy of 91.7%, sensitivity of 100%, specificity of 86.7%, and AUC of 0.96. For differentiation of benign from malignant parotid tumors, a threshold ADC value of (1.07×10^{-3} mm^2/s) was used with an accuracy of 77.1%, sensitivity of 88.9%, specificity of 70%, and AUC of 0.81 (Fig. 4A).

There was insignificant difference in the ADC value of malignant tumors ($0.94 \pm 0.20 \times 10^{-3}$ mm^2/s) and Warthin tumors ($0.94 \pm 0.08 \times 10^{-3}$ mm^2/s) with overlap in their ADC values. The DSC% of malignant tumors (33.53% ± 3.99) was significantly different from that of Warthin tumors (26.23% ± 4.44) ($P = 0.001$). The cutoff DSC% used for differentiation of malignant tumors from Warthin tumors was 26.9% with accuracy of 98%, sensitivity of 94%, specificity of 99%, and AUC of 0.98 (Fig. 4B).

The mean DSC% of pleomorphic adenomas was 20.11% ± 2.19%, and Warthin tumors was 26.23% ± 4.44%. There was significant difference ($P = 0.001$) in the DSC% of pleomorphic adenomas from Warthin tumors. The mean ADC value of pleomorphic adenomas was $1.35 \pm 0.11 \times 10^{-3}$ mm^2/s and significantly different ($P = 0.001$) from that of Warthin tumors ($0.94 \pm 0.08 \times 10^{-3}$ mm^2/s). When a DSC% of 22.5% was used as a threshold value for differentiating pleomorphic adenomas from Warthin tumors, the best result was obtained with an

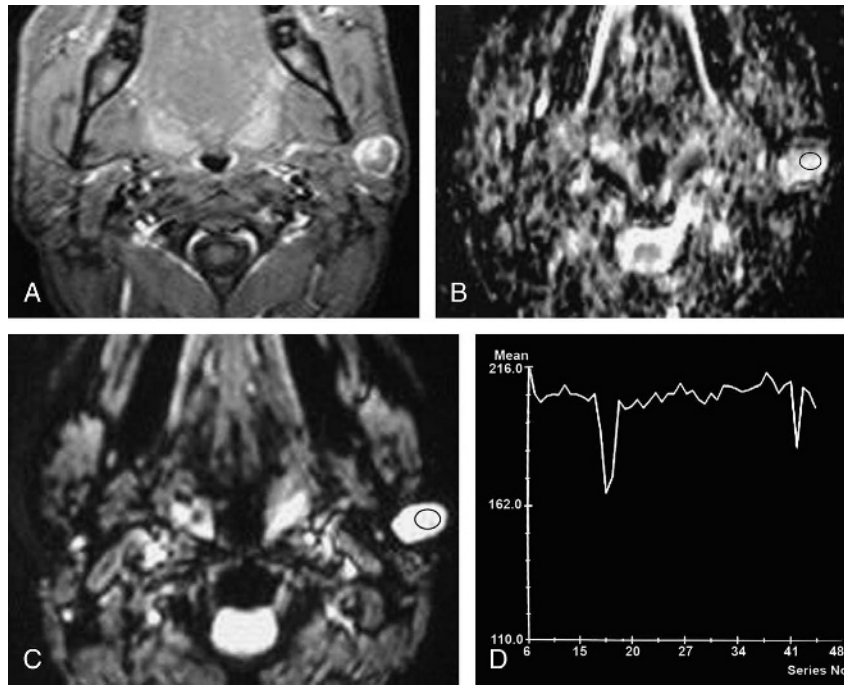

FIGURE 1. Pleomorphic adenoma. A, Axial contrast enhanced T1-weighted image shows enhancing mass in the superficial lobe of the left parotid gland. B, Axial ADC map shows unrestricted diffusion of the tumor with ADC value of 1.75×10^{-3} mm^2/s. C, Axial susceptibility perfusion-weighted MR image shows the ROI of the lesion, D, Time signal intensity curve shows the DSC% of the parotid tumor is 18.6%.

accuracy of 84.6%, sensitivity of 87.5%, specificity of 80%, and AUC of 0.88. The threshold ADC value of 0.99×10^{-3} mm^2/s was used for differentiation between both groups, with an accuracy of 96.2%, sensitivity of 100%, specificity of 90%, and AUC of 0.98 (Fig. 4C).

DISCUSSION

In this study, the main findings are that dynamic susceptibility contrast perfusion-weighted MR and diffusion-weighted MR imaging can help in differentiation of malignant from benign parotid tumors with accuracy of 91.7% and 77.1%, respectively, and AUC of 0.96 and 0.81, respectively, as well as in differentiation of pleomorphic adenomas from Warthin tumors with accuracy of 84.6% and 96.2% and AUC of 0.88 and 0.98, respectively. Dynamic susceptibly can differentiate malignant tumors from Warthin tumors with accuracy of 98% and AUC of 0.98.

In this study, DSC% of malignant parotid tumors is significantly different from that of benign tumors. This is attributed to the high vascularity with increased capillary perfusion of malignant parotid tumors compared with benign parotid tumors. The malignant tumor blood vessels are dilated and tortuous with no organization into the arterioles, capillaries, and venules. In addition, the size of the vessels increase with increased tumor angiogenesis. Several unique properties of new vessels include increased tumor blood volume, arteriovenous shunt formation, altered capillary transit time, and increased capillary permeability.[16–19] It is clinically important to preoperatively determine whether a salivary gland tumor is benign or malignant. Benign tumors undergo local excision or superficial parotidectomy, whereas malignant tumors are treated with total parotidectomy with or without facial nerve removal.[1–4]

In this study, there is significant difference in the ADC value between malignant and benign tumors. Different previous studies

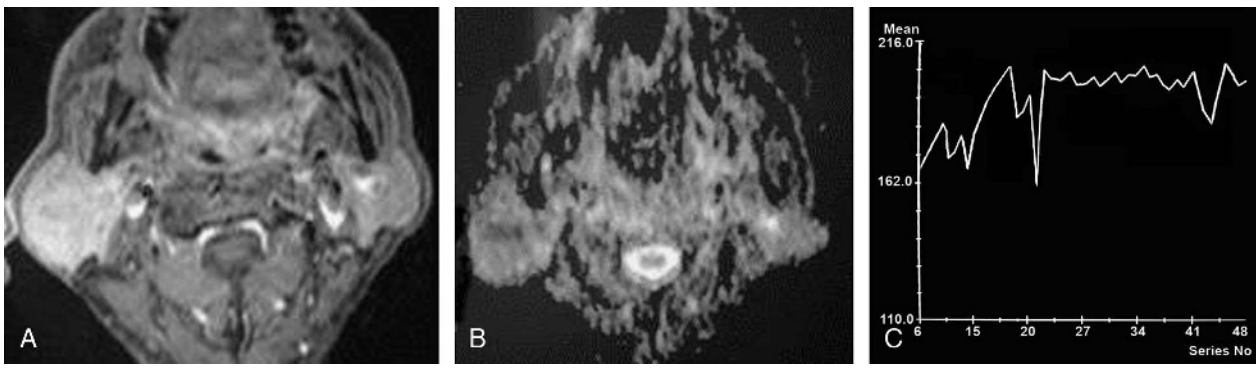

FIGURE 2. Warthin tumor. A, Axial contrast T1-weighted image shows enhancing soft tissue mass involving the superficial lobe of the right parotid gland. B, Axial ADC map shows restricted diffusion of the lesion with ADC value of 0.94×10^{-3} mm^2/s. C, Time signal intensity curve shows the DSC% of the parotid tumor is 21.2%.

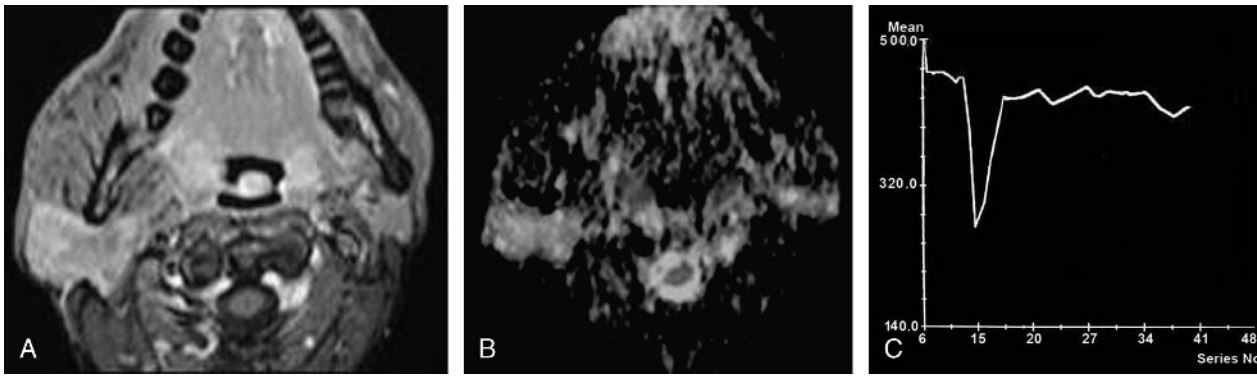

FIGURE 3. Mucoepidermoid carcinoma. A, Axial contrast T1-weighted image shows heterogeneously enhancing soft tissue mass involving the deep lobe of the right parotid gland. B, Axial ADC map shows restricted diffusion of the lesion with ADC value of 0.98×10^{-3} mm^2/s. C, Time signal intensity curve shows the DSC% of the lesion is 46.1%.

reported that there is overlap in the ADC values of benign and malignant tumors. They reported that mean ADCs of Warthin tumors were significantly lower than those of pleomorphic adenomas. However, they could not differentiate between benign and malignant tumors due to the overlap of ADC between Warthin tumors and malignant tumors.[20,22–25] This difference may be attributed to different histopathological subtypes of malignant and benign tumors and different parameters of diffusion-weighted MR imaging applied in different studies.

Differentiation of malignant tumors from Warthin tumors is a clinical dilemma because Warthin tumors require less aggressive surgical approach, whereas malignant tumors require superficial or total parotidectomy with or without facial nerve resection. Previous studies reported that there is overlap in ADC value of malignant parotid tumors with Warthin tumors. This is attributed to high cellularity of Warthin tumors.[21–24] In this study, there is insignificant difference in ADC values between Warthin tumors and malignancy with overlap in their values. However, dynamic susceptibility contrast perfusion-weighted MR imaging can help in this differentiation due to high vascularity and perfusion of malignant tumors compared with Warthin tumors.

Preoperative differentiation of Warthin tumors from pleomorphic adenomas is important because 25% of pleomorphic adenomas show malignant degeneration, in contrast to Warthin tumors, where malignant transformation is extremely rare (0.3%). Radical surgical excision is done in pleomorphic adenomas and limited partial parotidectomy or conservative observation is done in Warthin tumors is reliable. It has been estimated that 46% of Warthin tumors were reported as pleomorphic adenomas.[3–7]

In this study, dynamic susceptibility contrast perfusion-weighted MR imaging and diffusion-weighted MR imaging can differentiate pleomorphic adenoma from Warthin tumors. This could be attributed to the different vascularity, cellularity, and histopathological features of both tumors. Pleomorphic adenomas comprise the mesenchymal-like components of mucoid/myxoid, cartilaginous, or hyalinized materials as products of myoepithelial cells. The tumor areas with myxomatous or fibrous connective tissues have tended to exhibit relatively higher DSC%. On the other hand, Warthin tumors comprise varying proportions of oncocytic epithelium and lymphoid stroma. The dense lymphoid stroma often looks similar to a normal lymph node, complete with lymphoid follicles and germinal centers. The tumor areas of hypercellularity, such as the densely packed lymphoid tissue of Warthin tumors responsible for lower ADC value and less vascularity compared with pleomorphic adenomas.[20,22–26]

In this work, we applied semiquantitative analysis of time intensity curve with calculation of DSC%. Applications of advanced postprocessing techniques with creation of parametric maps, such as tumor blood flow map and tumor blood volume, will improve the results. In addition, application of advanced postprocessing of diffusion-weighted MR imaging at higher 3 Tesla, such as diffusion kurtosis, will improve the results.[27,28]

There are few limitations of this study. First, the patient population studied is very diverse which included both malignant and

TABLE 1. Mean and Standard Deviation of DSC% and ADC Values of Parotid Tumors

Type	No	DSC%	ADC (10^{-3} mm^2/s)
Benign parotid tumors	30	22.29 ± 4.13 (18.1–26.4)	1.2 ± 0.22 (0.9–1.4)
Pleomorphic adenoma	16	20.11 ± 2.19 (17.9–22.3)	1.35 ± 1.16 (0.2–2.5)
Warthin's tumors	10	26.23 ± 4.44 (21.2–30.6)	0.94 ± 0.08 (0.8–1.1)
Neurofibroma	2	21.70 ± 0.70 (21.0–22.4)	1.41 ± 0.04 (1.3–1.4)
Monomorphic adenoma	2	20.70 ± 2.82 (17.8–23.5)	1.38 ± 0.05 (1.3–1.4)
Malignant parotid tumors	18	33.53 ± 3.99 (29.5–37.5)	0.94 ± 0.22 (0.7–1.2)
Muco-epidermoid carcinoma	8	35.11 ± 3.16 (31.9–38.3)	0.94 ± 0.08 (0.8–1.1)
Adenoid cystic carcinoma	2	28.05 ± 2.05 (26.0–30.1)	1.46 ± 0.03 (1.4–1.4)
Carcinoma ex adenoma	2	34.20 ± 6.50 (27.7–40.7)	0.82 ± 0.01 (0.8–0.8)
Non-Hodgkin lymphoma	4	31.20 ± 3.18 (28.1–34.4)	0.80 ± 0.05 (0.7–0.8)
Metastasis	2	36.70 ± 0.70 (36.0–37.4)	0.85 ± 0.05 (0.80–0.90)

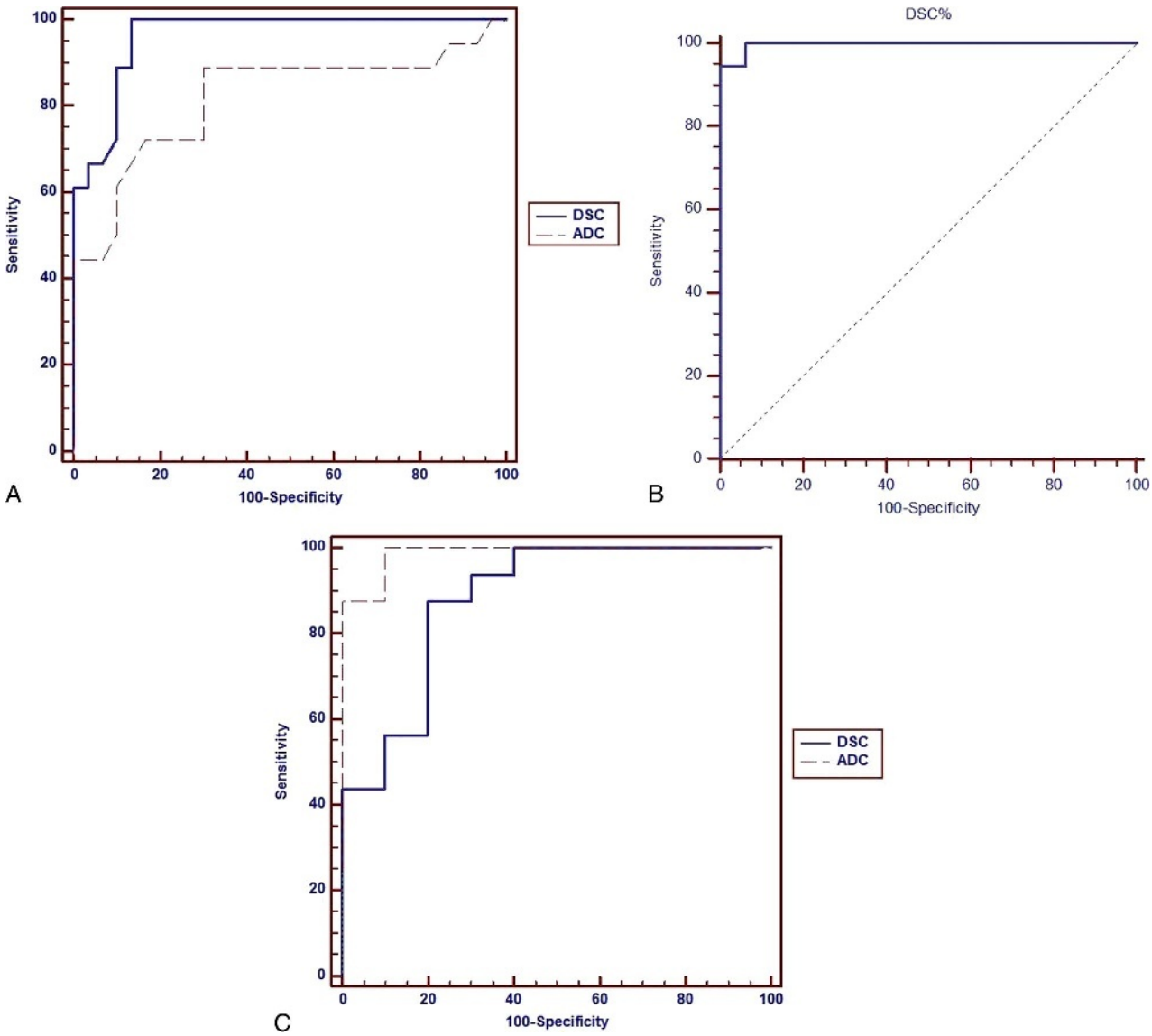

FIGURE 4. ROC curves. A, ROC of DSC% and ADC used to differentiate malignant from benign parotid tumors with the area under curve is 0.96 and 0.81, respectively. B, ROC of DSC% used to differentiate malignant tumors from Warthin's tumors with the area under curve is 0.98. C, ROC of DSC% and ADC used to differentiate pleomorphic adenomas from Warthin tumors with the area under curve is 0.88 and 0.98, respectively. ROC, receiver operating characteristic. Figure 4 can be viewed online in color at www.jcat.org.

benign parotid tumors. The biological behavior and vascularity of these tumors are also quite diverse. Even the age of the patient is variable ranging from 15 to 75 years. Further studies that include more homogenous study samples in a specific age group are required to address the impact of these variables on the signal intensity reduction. Second, the statistical sample size in each category is still small to arrive at a meaningful result. Third, we analyze image depending upon time signal intensity curve, application of advanced software with calculation of the tumor blood volume, and arterial spin labeling of parotid gland with calculation of tumor blood flow map is recommended.[26]

CONCLUSIONS

We concluded that dynamic susceptibility contrast-enhanced perfusion-weighted MR imaging and diffusion-weighted MR imaging are noninvasive promising methods that can be used for differentiation of malignant from benign parotid tumors and characterization of some benign parotid tumors.

REFERENCES

1. Bag AK, Curé JK, Chapman PR, et al. Practical imaging of the parotid gland. *Curr Probl Diagn Radiol*. 2015;44:167–192.
2. Prasad RS. Parotid gland imaging. *Otolaryngol Clin North Am*. 2016; doi: 10.1016/j.otc.2015.10.003.
3. Lethaus B, Ketelsen D, van Stiphout R, et al. MR imaging of salivary glands tumours. *Rofo*. 2011;183:203–207.
4. Abdel Razek AA, Ashmalla GA, Gaballa G, et al. Pilot study of ultrasound Parotid Imaging Reporting and Data System (PIRADS): inter-observer agreement. *Eur J Radiol*. 2015;84:2533–2538.

5. Wu S, Liu G, Chen R, et al. Role of ultrasound in the assessment of benignity and malignancy of parotid masses. *Dentomaxillofac Radiol*. 2012;41:131–135.
6. Celebi I, Mahmutoglu AS. Early results of real-time qualitative sonoelastography in the evaluation of parotid gland masses: a study with histopathological correlation. *Acta Radiol*. 2013;54:35–41.
7. Dong Y, Lei GW, Wang SW, et al. Diagnostic value of CT perfusion imaging for parotid neoplasms. *Dentomaxillofac Radiol*. 2013; 43:20130237.
8. Razek AA, Tawfik AM, Elsorogy LG, et al. Perfusion CT of head and neck cancer. *Eur J Radiol*. 2014;83:537–544.
9. Christe A, Waldherr C, Hallett R, et al. MR imaging of parotid tumors: typical lesion characteristics in MR imaging improve discrimination between benign and malignant disease. *AJNR Am J Neuroradiol*. 2011;32:1202–1207.
10. Lam PD, Kuribayashi A, Imaizumi A, et al. Differentiating benign and malignant salivary gland tumours: diagnostic criteria and the accuracy of dynamic contrast-enhanced MRI with high temporal resolution. *Br J Radiol*. 2015;88:20140685.
11. Yuan Y, Tang W, Tao X. Parotid gland lesions: separate and combined diagnostic value of conventional MRI, diffusion-weighted imaging and dynamic contrast-enhanced MRI. *Br J Radiol*. 2016;89:20150912.
12. Abdel Razek AA, Poptani H. MR spectroscopy of head and neck cancer. *Eur J Radiol*. 2013;82:982–989.
13. King A, Yeung D, Ahuja A, et al. Salivary gland tumors at in vivo proton MR spectroscopy. *Radiology*. 2005;237:563–569.
14. Welker K, Boxerman J, Kalnin A, et al. ASFNR recommendations for clinical performance of MR dynamic susceptibility contrast perfusion imaging of the brain. *AJNR Am J Neuroradiol*. 2015;36:E41–E51.
15. Calamante F. Perfusion MRI using dynamic-susceptibility contrast MRI: quantification issues in patient studies. *Top Magn Reson Imaging*. 2010;21:75–85.
16. Abdel Razek AA, Gaballa G. Role of perfusion magnetic resonance imaging in cervical lymphadenopathy. *J Comput Assist Tomogr*. 2011;35:21–25.
17. Wu R, Bruening R, Ducreux D, et al. Estimation of relative blood volume in head and neck squamous cell carcinomas. *J Neuroradiol*. 2004;31:190–197.
18. Razek AA, Elsorogy LG, Soliman NY, et al. Dynamic susceptibility contrast perfusion MR imaging in distinguishing malignant from benign head and neck tumors: a pilot study. *Eur J Radiol*. 2011;77:73–79.
19. Abdel Razek AA, Gaballa G, Ashamalla G, et al. Dynamic susceptibility contrast perfusion-weighted magnetic resonance imaging and diffusion-weighted magnetic resonance imaging in differentiating recurrent head and neck cancer from postradiation changes. *J Comput Assist Tomogr*. 2015;39:849–854.
20. Habermann CR, Arndt C, Graessner J, et al. Diffusion-weighted echo-planar MR imaging of primary parotid gland tumors: is a prediction of different histologic subtypes possible? *AJNR Am J Neuroradiol*. 2009;30:591–596.
21. Razek AA. Diffusion-weighted magnetic resonance imaging of head and neck. *J Comput Assist Tomogr*. 2010;34:808–815.
22. Eida S, Sumi M, Sakihama N, et al. Apparent diffusion coefficient mapping of salivary gland tumors: prediction of the benignancy and malignancy. *AJNR Am J Neuroradiol*. 2007;28:116–121.
23. Lechner Goyault J, Riehm S, Neuville A, et al. Interest of diffusion-weighted and gadolinium-enhanced dynamic MR sequences for the diagnosis of parotid gland tumors. *J Neuroradiol*. 2011;38:77–89.
24. Eida S, Sumi M, Nakamura T. Multiparametric magnetic resonance imaging for the differentiation between benign and malignant salivary gland tumors. *J Magn Reson Imaging*. 2010;31:673–679.
25. Yabuuchi H, Matsuo Y, Kamitani T, et al. Parotid gland tumors: can addition of diffusion-weighted MR imaging to dynamic contrast enhanced MR imaging improve diagnostic accuracy in characterization? *Radiology*. 2008;249:909–916.
26. Kato H, Kanematsu M, Watanabe H, et al. Perfusion imaging of parotid gland tumours: usefulness of arterial spin labeling for differentiating Warthin's tumours. *Eur Radiol*. 2015;25:3247–3254.
27. Razek AA, Elkhamary S, Mousa A. Differentiation between benign and malignant orbital tumors at 3-T diffusion MR-imaging. *Neuroradiology*. 2011;53:517–522.
28. Razek AA, Nada N. Correlation of choline/creatine and apparent diffusion coefficient values with the prognostic parameters of head and neck squamous cell carcinoma. *NMR Biomed*. 2016; DOI: 10.1002/nbm.3472.